

OPG-Fc but Not Zoledronic Acid Discontinuation Reverses Osteonecrosis of the Jaws (ONJ) in Mice

Rafael Scaf de Molon,^{1,2} Hiroaki Shimamoto,³ Olga Bezouglia,¹ Flavia Q Pirih,⁴ Sarah M Dry,⁵ Paul Kostenuik,⁶ Rogely W Boyce,⁷ Denise Dwyer,⁷ Tara L Aghaloo,¹ and Sotirios Tetradis^{1,8}

¹Division of Diagnostic and Surgical Sciences, UCLA School of Dentistry, Los Angeles, CA, USA

²Department of Diagnosis and Surgery, School of Dentistry at Araraquara, São Paulo State University, Araraquara, Brazil

³Department of Oral and Maxillofacial Radiology, Osaka University Graduate School of Dentistry, Osaka, Japan

⁴Division of Associated Specialties, UCLA School of Dentistry, Los Angeles, CA, USA

⁵Department of Pathology and Laboratory Medicine, David Geffen School of Medicine at UCLA, Los Angeles, CA, USA

⁶Department of Periodontics and Oral Medicine, School of Dentistry, University of Michigan, Ann Arbor, MI, USA

⁷Department of Comparative Biology and Safety Sciences, Amgen Inc., Thousand Oaks, CA, USA

⁸Molecular Biology Institute, UCLA, Los Angeles, CA, USA

ABSTRACT

Osteonecrosis of the jaws (ONJ) is a significant complication of antiresorptive medications, such as bisphosphonates and denosumab. Antiresorptive discontinuation to promote healing of ONJ lesions remains highly controversial and understudied. Here, we investigated whether antiresorptive discontinuation alters ONJ features in mice, employing the potent bisphosphonate zoledronic acid (ZA) or the receptor activator of NF- κ B ligand (RANKL) inhibitor OPG-Fc, utilizing previously published ONJ animal models. Mice were treated with vehicle (veh), ZA, or OPG-Fc for 11 weeks to induce ONJ, and antiresorptives were discontinued for 6 or 10 weeks. Maxillae and mandibles were examined by μ CT imaging and histologically. ONJ features in ZA and OPG-Fc groups included periosteal bone deposition, empty osteocyte lacunae, osteonecrotic areas, and bone exposure, each of which substantially resolved 10 weeks after discontinuing OPG-Fc but not ZA. Full recovery of tartrate-resistant acid phosphatase-positive (TRAP+) osteoclast numbers occurred after discontinuing OPG-Fc but not ZA. Our data provide the first experimental evidence demonstrating that discontinuation of a RANKL inhibitor, but not a bisphosphonate, reverses features of osteonecrosis in mice. It remains unclear whether antiresorptive discontinuation increases the risk of skeletal-related events in patients with bone metastases or fracture risk in osteoporosis patients, but these preclinical data may nonetheless help to inform discussions on the rationale for a “drug holiday” in managing the ONJ patient. © 2015 American Society for Bone and Mineral Research.

KEY WORDS: OSTEONECROSIS OF THE JAW (ONJ); ANTIRESORPTIVES; BISPHOSPHONATES; ZOLEDRONIC ACID; DENOSUMAB; ALVEOLAR BONE; OSTEOCLASTS

Introduction

Antiresorptive medications, such as bisphosphonates (BPs) and the receptor activator of NF- κ B ligand (RANKL) inhibitor denosumab impede osteoclastic bone resorption and are used in the clinic to manage bone diseases, such as primary or metastatic bone malignancy and osteoporosis. These medications, studied in cancer and postmenopausal women with osteoporosis populations, reduce skeletal-related events (SREs), decrease tumor burden, reduce bone pain, decrease incidence of osteoporotic fractures, and help improve patients' quality of life.^(1–4) Despite their distinctly different pharmacologic mechanism of action, BPs and denosumab are each associated with osteonecrosis of the jaw (ONJ), an infrequent but serious adverse

effect, particularly when administered at high doses.⁽⁵⁾ Antiresorptive-related ONJ is defined as exposed bone or bone that can be probed through an intraoral or extraoral fistula in the maxillofacial region that has persisted for more than 8 weeks in patients on current or previous treatment with antiresorptive agents and no history of radiation therapy to the jaws or obvious metastatic disease to the jaws.^(6–8) The term medical-related ONJ (MRONJ) was recently introduced to include ONJ cases associated with antiangiogenic therapies.⁽⁷⁾

Although ONJ has been described for more than a decade,^(9,10) the etiology and pathogenesis of the disease remain largely unknown.^(5,11–13) Osteoclast inhibition and bone remodeling suppression, inflammation and/or infection, inhibition of angiogenesis, soft tissue toxicity, and altered immune cell

Received in original form January 26, 2015; revised form February 20, 2015; accepted February 24, 2015; accepted manuscript online February 28, 2015.

Address correspondence to: Sotirios Tetradis, DDS, PhD, UCLA School of Dentistry, 10833 Le Conte Avenue, CHS Room 53-068, Los Angeles, CA 90095-1668, USA. E-mail: stetradis@dentistry.ucla.edu. Tara L Aghaloo, DDS, MD, PhD, UCLA School of Dentistry, 10833 Le Conte Avenue, CHS Room 53-009, Los Angeles, CA 90095-1668, USA. E-mail: taghaloo@dentistry.ucla.edu

Additional Supporting Information may be found in the online version of this article.

Journal of Bone and Mineral Research, Vol. 30, No. 9, September 2015, pp 1627–1640

DOI: 10.1002/jbmr.2490

© 2015 American Society for Bone and Mineral Research

function are among the hypotheses proposed to underlie ONJ development and progression.^(5,11–13) Clinical observations and experimental findings provide support for several of these hypotheses, suggesting that ONJ is probably a multifactorial disease influenced by many variables.⁽⁷⁾

Because antiresorptive medications with distinct pharmacologic function induce similar incidence of ONJ, osteoclastic inhibition and bone turnover suppression appear central in antiresorptive-related ONJ.^(5,11–13) To that effect, discontinuation of antiresorptive treatment before tooth extraction or other dental surgical intervention or after ONJ development has been proposed as potentially beneficial in improving osteoclast function recovery, which could, in turn, increase bone turnover and improve bone healing.^(7,14–16) However, such recommendations have only a theoretical basis, and clinical or experimental data supporting the benefit of antiresorptive drug withdrawal in preventing ONJ development or promoting resolution are lacking.^(7,17) Furthermore, the consequences of such “drug holidays” on the progression of SREs in cancer patients or fragility fractures in osteoporosis patients remain unclear. As such, an important first step in informing treatment planning decisions is to understand whether discontinuation of antiresorptive treatments mitigates the risk of developing ONJ or fosters the resolution of established ONJ.^(7,8)

Animal models recapitulating ONJ-like lesions in mice, rats, minipigs, and dogs treated with bisphosphonates have provided important insights into ONJ pathophysiology.^(18–29) Moreover, utilizing OPG-Fc and RANK-Fc as surrogates for denosumab,⁽³⁰⁾ we reported for the first time ONJ-like lesions

in the presence of periapical disease or spontaneous periradicular inflammation in mice treated with the RANKL inhibitors,^(31,32) thus supporting the central role of osteoclastic inhibition in ONJ pathogenesis. Similar ONJ-like changes were reported more recently in mice that underwent tooth extractions and were treated with an antibody against mouse RANKL.⁽³³⁾

In this study, utilizing ONJ animal models, we explored the effects of zoledronic acid (ZA) or OPG-Fc discontinuation on radiographic and histologic features of established ONJ in mice. Our findings indicate that, within the experimental time frame, OPG-Fc but not ZA discontinuation reversed features of osteonecrosis in ONJ animal models.

Materials and Methods

Animal care

Mice and surgical procedures were handled according to the guidelines of the Institutional Animal Care and Use Committee of the University of California, Los Angeles. We followed a randomized, prospective, controlled, animal model design following all the recommendations of the ARRIVE (Animal Research: Reporting In Vivo Experiments) guidelines for the execution and submission of studies in animals (Kilkenny and colleagues). Mice were kept in the animal facilities with controlled temperature ($23^{\circ}\text{C} \pm 2^{\circ}\text{C}$), humidity, and a 12-hour light/dark cycle. Throughout the experimental period, mice were housed in plastic cages, fed a standard laboratory

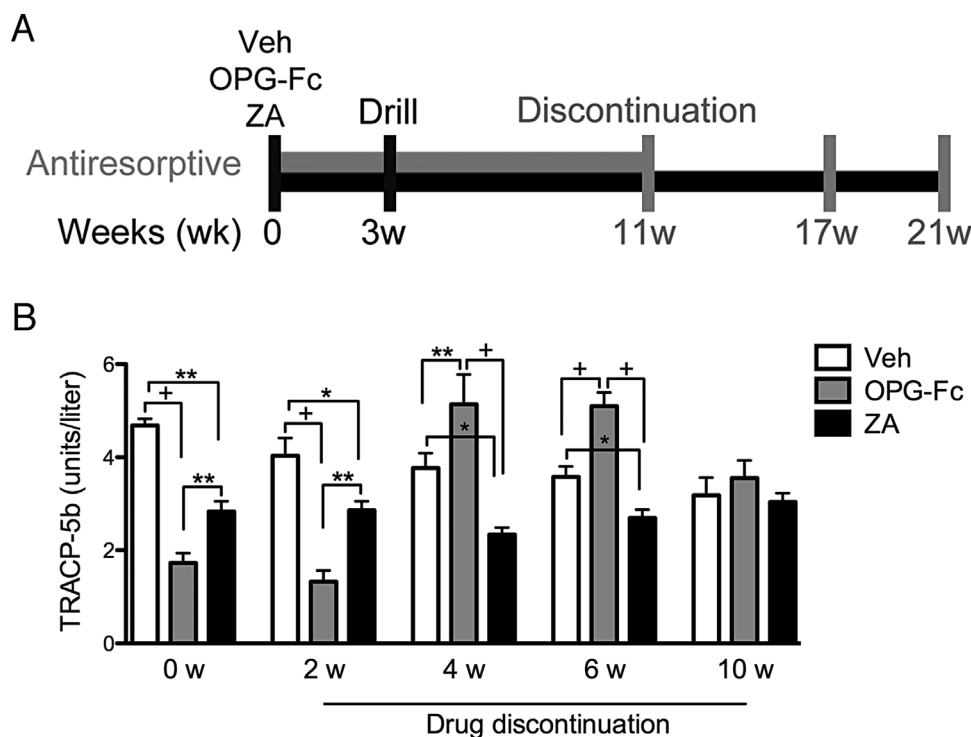


Fig. 1. Serum TRACP-5b levels increase after OPG-Fc but not after ZA discontinuation. TRACP-5b serum levels were measured at the end of treatment (0 weeks) and 2, 4, 6, and 10 weeks after drug discontinuation (13, 15, 17, and 21 weeks after the first injection) ($n = 16/\text{group}$ per period). ⁺Statistically significantly different from indicated groups, $p < 0.0001$. ^{**}Statistically significantly different from indicated groups, $p < 0.001$. ^{*}Statistically significantly different from indicated groups, $p < 0.05$.

Table 1. Summary of Radiographic and Histologic Findings on Various Groups and Experimental Time Points

Group	Total no. of hemimandible and hemimaxillae	Healthy (%)	Diseased (%)	Osteonecrosis (%)	Bone exposure (%)
Veh 11w	64	34 (53) ^a	30 (47) ^a	0 ^d (0) ^a (0) ^b	0 ^f (0) ^a (0) ^b (0) ⁺
Veh 17w	64	31 (48) ^a	33 (52) ^a	2 ^e (3.1) ^a (6) ^b	0 ^d (0) ^a (0) ^b (0) ^c
Veh 21w	64	26 (40) ^a	38 (60) ^a	1 ^e (1.5) ^a (2.6) ^b	0 ^d (0) ^a (0) ^b (0) ^c
OPG-Fc 11w	64	32 (50) ^a	32 (50) ^a	24 (37.5) ^a (75) ^b	13 (20.3) ^a (40.6) ^b (54.2) ^c
OPG-Fc 17w	64	26 (40) ^a	38 (60) ^a	16 ^g (25) ^a (42.1) ^b	3 ^d (4.7) ^a (7.9) ^b (18.7) ^c
OPG-Fc 21w	64	24 (37) ^a	40 (63) ^a	13 ^g (20.3) ^a (32.5) ^b	0 ^d (0) ^a (0) ^b (0) ^c
ZA 11w	64	34 (53) ^a	30 (47) ^a	19 (29.7) ^a (63.4) ^b	10 (15.6) ^a (33.3) ^b (52.6) ^c
ZA 17w	64	27 (42) ^a	37 (58) ^a	32 (50) ^a (86.5) ^b	19 (29.7) ^a (51.4) ^b (59.3) ^c
ZA 21w	64	23 (36) ^a	41 (64) ^a	31 (48.4) ^a (75.6) ^b	21 (32.8) ^a (51.2) ^b (67.7) ^c

^aPercent of total hemimaxillae and hemimandible.

^bPercent of diseased hemimaxillae and hemimandible.

^cPercent of hemimaxillae and hemimandible with osteonecrosis.

^dStatistically significantly different, $p < 0.05$ compared with OPG-Fc and ZA.

^eStatistically significantly different, $p < 0.0001$ compared with OPG-Fc and ZA.

^fStatistically significantly different, $p < 0.005$ compared with OPG-Fc and ZA.

^gStatistically significantly different, $p < 0.0001$ compared with ZA.

diet, and given water *ad libitum*. A total of 144 10-week-old C57BL/6J wild-type male mice (Jackson Laboratories, Bar Harbor, ME, USA) with average weight of 25 g were randomly divided into three experimental groups of 48 animals that received intraperitoneal (ip) injections of endotoxin-free saline (group veh) two times per week, 10 mg/kg rat OPG-Fc (composed of the RANKL-binding domains of osteoprotegerin linked to the Fc portion of IgG,^(32,34,35) kindly provided by Amgen, Inc, Thousand Oaks, CA, USA) twice per week (group OPG-Fc), or 200 μ g/kg zoledronic acid (Z-5744, LKT Laboratories, St. Paul, MN, USA) twice per week (group ZA). These doses were

used to increase the incidence of ONJ-like lesions in the mice, as described previously.

Periapical disease induction

Experimental periapical disease was performed as described.^(29,32,36,37) Briefly, the crowns of the right mandibular 1st and 2nd molars were drilled utilizing a stainless-steel ¼ size round bur in a high-speed handpiece, avoiding furcal perforation, and the root canals were left exposed to the oral environment, resulting in pulpal necrosis and subsequent

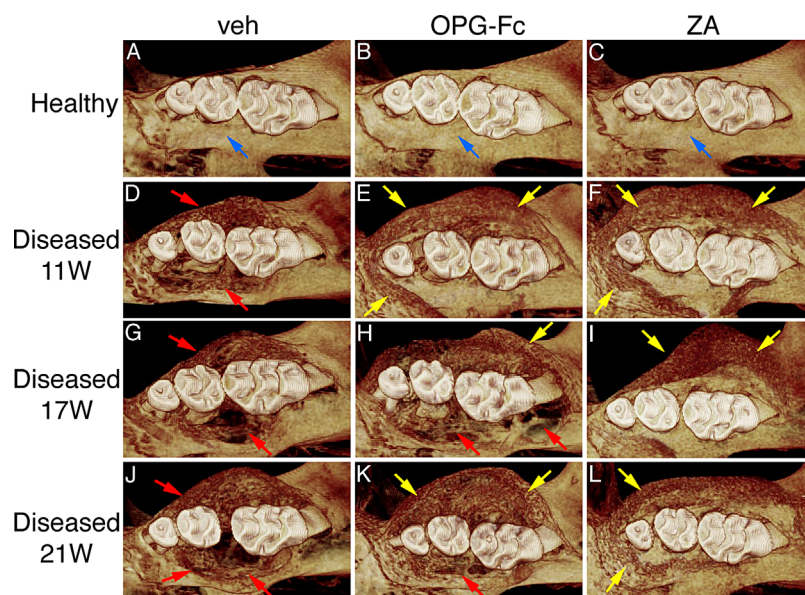


Fig. 2. Three-dimensional μ CT reconstructed images of maxilla. (A–C) Healthy site in veh, OPG-Fc, and ZA, respectively. (D, E) Diseased site after 11 weeks of treatment. (G–L) Diseased site at 6 and 10 weeks after drug discontinuation. Blue arrows point to normal alveolar bone crest in the interproximal area between the distal root of the first molar and mesial root of the second molar. Red arrows point to periodontal bone loss and areas of osteolysis in the diseased site of OPG-Fc- and veh-treated mice. Yellow arrows point to increased bone deposition.

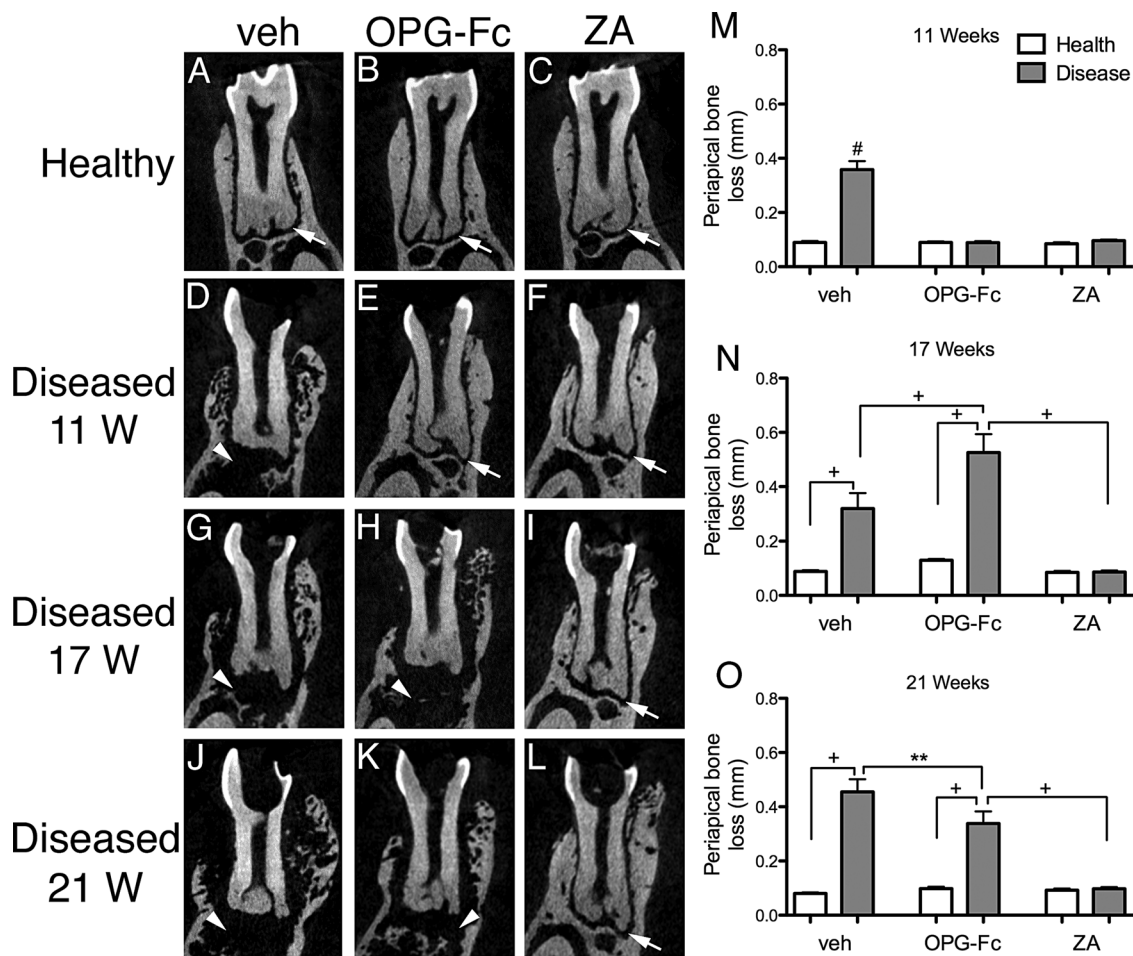


Fig. 3. μ CT cross sections of the periapical area of first molars from animals treated with veh, OPG-Fc, and ZA followed by drug discontinuation. (A–C) Nondrilled molars at 11 weeks. (D–F) Drilled molars at 11 weeks. (G–I) Drilled molars 6 weeks after drug discontinuation. (J–L) Drilled molars 10 weeks after drug discontinuation ($n = 16/\text{group}$ per period). Thin arrows point to normal PDL space. Arrowheads point to periapical bone loss. (M–O) Quantification of periapical bone loss at the distal root of the first molar and mesial root of the second molar. [#]Statistically significantly different compared with all other groups, $p < 0.0001$. ⁺Statistically significantly different from indicated groups, $p < 0.0001$. ^{**}Statistically significantly different from indicated groups, $p < 0.001$.

periapical infection. The crowns of the left 1st and 2nd molars were kept intact.

Spontaneous naturally occurring maxillofacial abscesses

Naturally occurring, spontaneous maxillofacial abscesses have been described in mice.⁽³⁸⁾ Hair inserts into the gingival sulcus and results in bacterial colonization and reproducible, severe periradicular osteolysis.^(38–40) Such diseased maxillary sites, identified by periradicular osteolysis by μ CT imaging, were compared with sites with healthy dento-alveolar structures.⁽³¹⁾

Antiresorptive administration and serum TRACP-5b measurement

Mice were pretreated with veh, OPG-Fc, or ZA for 3 weeks, and periapical disease was induced. Animals continued to receive veh, OPG-Fc, and ZA for 8 additional weeks, after which antiresorptives were discontinued (Fig. 1A). Blood was collected via retro-orbital bleeding after 11 weeks of the experiment (at

the end of antiresorptives treatment) and 2, 4, 6, and 10 weeks after antiresorptive withdrawal. Serum tartrate-resistant acid phosphatase 5b (TRACP-5b) was measured by enzyme immunoassay (RatTRAP; JDS, Gaithersburg, MD, USA).

Animal euthanization and analyses

Sixteen mice from each of the veh, OPG-Fc, and ZA groups were euthanized via isoflurane overdose at 11 weeks (time of antiresorptive discontinuation), at 17 weeks (6 weeks after discontinuation), and at 21 weeks (10 weeks after antiresorptive discontinuation). The maxillae, mandibles, and femurs were fixed in 4% paraformaldehyde for 48 hours and stored in 70% ethanol.

Micro-computed tomography (μ CT) scanning

Maxillae and mandibles were imaged using a μ CT scanner (μ CT Skyscan 1172; Skyscan, Kontich, Belgium) at 10 μm resolution, as described.^(29,32) For linear measurements, axial slices were converted to DICOM format and imported in the Dolphin

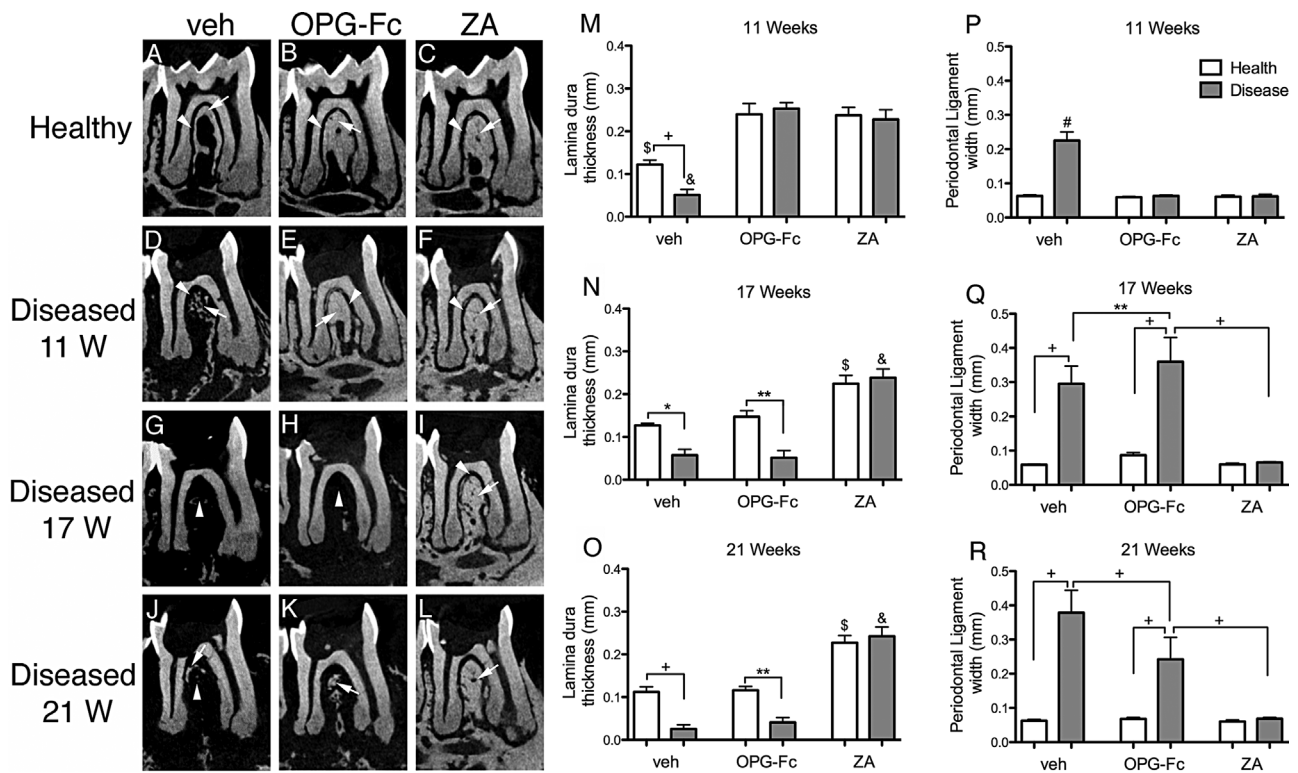


Fig. 4. Sagittal μ CT sections through the furcational periodontium of veh-, OPG-Fc-, and ZA-treated animals. (A–C) Nondrilled molars at 11 weeks. (D–F) Drilled molars at 11 weeks. (G–I) Drilled molars 6 weeks after drug discontinuation. (J–L) Drilled molars 10 weeks after drug discontinuation ($n = 16$ /group per period). Thin arrows point to lamina dura and arrowheads point to PDL space. (M–R) Quantification of changes in the furcational periodontium was performed measuring the thickness of lamina dura and width of the PDL space. [§]Statistically significantly different compared with healthy mice, $p < 0.0001$. [&]Statistically significantly different compared with diseased mice, $p < 0.0001$. ⁺Statistically significantly different from indicated groups, $p < 0.0001$. ^{**}Statistically significantly different from indicated groups, $p < 0.001$. ^{*}Statistically significantly different from indicated groups, $p < 0.05$.

Imaging software (Chatsworth, CA, USA). Periapical bone loss, lamina dura thickness, periodontal ligament (PDL) space width, lingual bone thickness, and cemento-enamel junction (CEJ) to alveolar bone crest (ABC) distance were measured as described.^(29,31,32) Bone volume (BV), tissue volume (TV), and bone volume fraction (BV/TV) of the alveolar were measured using the CTAn software (Skyscan).

Femurs were imaged utilizing the μ CT scanner at 12 μ m resolution. Starting 100 μ m proximal to the distal growth plate, 200 axial slices were selected. BV, TV, BV/TV, trabecular number (Tb.N), trabecular thickness (Tb.Th), and trabecular spacing (Tb.Sp) were determined using the CTAn software. The measurement terminology and units used for μ CT analysis were those recommended by the Nomenclature Committee of the American Society for Bone and Mineral Research.⁽⁴¹⁾

Histology and TRAP staining

Mandibles, maxillae, and femurs were decalcified in 14.5% EDTA for 3 weeks and paraffin embedded, and 5 μ m sections were obtained. Hematoxylin and eosin (H&E)-stained sections were digitally scanned using the Aperio AT automated slide scanner (Aperio Technologies, Inc, Vista, CA, USA). Using the ruler tool in Aperio ImageScope software, the crestal 1 mm of the alveolar bone was marked and all measurements were performed in this area for mandible and maxilla.

The epithelium to alveolar crest distance was measured in the palatal side of the maxilla and in the lingual side of the mandible. The number of osteocytic lacunae and empty osteocytic lacunae and the total bone area and osteonecrotic area (defined as five or more contiguous empty osteocytic lacunae) were measured. To quantify periosteal bone thickness, the Aperio ruler tool was used to measure the three greatest areas of the buccal periosteal thickness that were then averaged.

To quantify osteoclast number, sections of the mandible, maxilla, and femur were stained using the leukocyte acid phosphatase kit (Sigma-Aldrich, St. Louis, MO, USA) and TRAP+ cells adjacent to the bone surface were counted. TRAP+ cells were measured for 8 mice per group. All histology and digital imaging were performed at the Translational Pathology Core Laboratory (TPCL) at UCLA.

Statistics

Analyses were performed using GraphPad Prism Software (GraphPad Software, Inc, La Jolla, CA, USA). Group measures were expressed as mean \pm the standard error of the mean (SEM). Statistical significance was assessed using one-way analysis of variance (ANOVA) followed by post hoc Tukey's test for multiple comparisons among groups. Data between groups (healthy versus diseased) were compared using the Student's t test. Categorical data (Table 1) were analyzed using the Fisher's exact test.

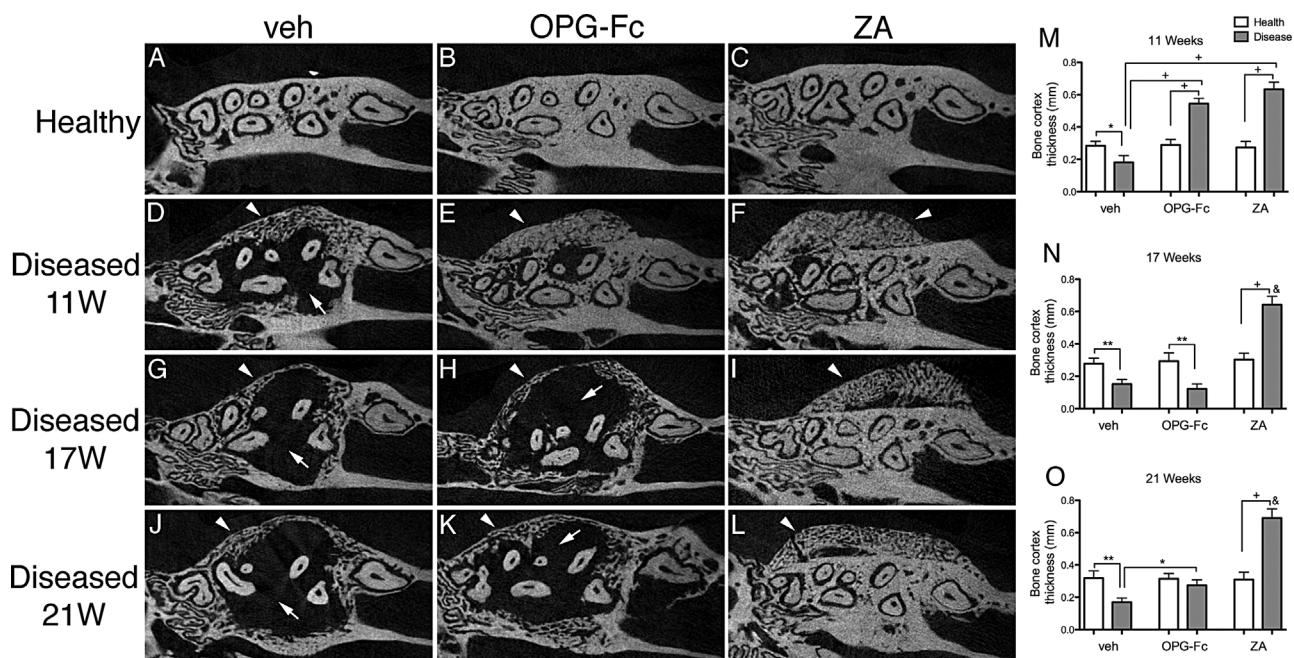


Fig. 5. Axial μ CT sections through the maxillary alveolar ridge. (A–C) Healthy maxillae at 11 weeks. (D–F) Diseased maxillae 11 weeks after drug discontinuation. (G–I) Diseased maxillae 6 weeks after drug discontinuation. (J–L) Diseased maxillae 10 weeks after drug discontinuation ($n = 16/\text{group}$ per period). Thin arrows point to areas of osteolysis. Arrowheads point to bone deposition and bone expansion. (M–O) Quantification of buccal bone thickness. †Statistically significantly different compared with diseased mice, $p < 0.0001$. ‡Statistically significantly different from indicated groups, $p < 0.0001$. **Statistically significantly different from indicated groups, $p < 0.001$. *Statistically significantly different from indicated groups, $p < 0.05$.

Results

Serum TRACP-5b levels increased after OPG-Fc but not after ZA discontinuation

Serum TRACP-5b levels were measured at the end of antiresorptive treatment (0 weeks: immediately after the last injection and 11 weeks after the beginning of the experiment), and 2, 4, 6, and 10 weeks after drug discontinuation (13, 15, 17, and 21 weeks after the beginning of the experiment). For the veh group, serum TRACP-5b levels remained relatively steady with a slight decline over time. After 11 weeks of treatment, ZA or OPG-Fc significantly decreased serum TRACP-5b levels in all animals, confirming the inhibition of osteoclastic function and absence of neutralizing antibody production to OPG-Fc.⁽⁴²⁾ These TRACP-5b levels remained unchanged for all groups 2 weeks after antiresorptive discontinuation. Interestingly, by 4 to 6 weeks post-OPG-Fc discontinuation, TRACP-5b rose above baseline and then returned to baseline by 10 weeks. TRACP-5b post-ZA discontinuation remained at reduced levels for 4 to 6 weeks and progressively returned to baseline by 10 weeks (Fig. 1B).

OPG-Fc but not ZA discontinuation reversed radiographic features of ONJ

The effect of antiresorptives and drug discontinuation on maxilla, mandible, and femur was assessed by μ CT. Healthy maxillae in all groups showed normal alveolar crest extending immediately below the cemento-enamel junction (CEJ), covering most of the root and the 1st and 2nd molar root furcation and absence of bone resorption and/or bone expansion (Fig. 2A–C; Supplemental Fig. S1A–C). In contrast, diseased

veh-treated mice showed altered alveolar bone morphology with large loss of alveolar crest height; bone loss covering the 1st, 2nd, and 3rd molars that in the majority of animals extended almost to the root apex surrounding the entire root; and significant buccal and palatal bone expansion of the alveolar ridge. These changes were similar for all time points (Fig. 2D, G, J; Supplemental Fig. S1D, G, J). In the diseased site of OPG-Fc- and ZA-treated mice, bone loss was also present. However, the extent of bone loss was significantly decreased and was associated with large areas of periosteal bone apposition in the buccal and palatal side of the maxillae that resulted in substantial bone expansion (Fig. 2E, F; Supplemental Fig. S1E, F). Discontinuation for 6 or 10 weeks of OPG-Fc but not ZA reversed these effects, such that the OPG-Fc and veh groups appeared similar and distinct from the ZA group (Fig. 2H, I, K, L; Supplemental Fig. S1H, I, K, L). Similar findings were observed for the mandibular alveolar ridge in nondrilled and drilled sites of veh, OPG-Fc-, and ZA-treated animals (Supplemental Fig. S2).

We then quantified radiographic changes among the various groups.^(29,32) In the nondrilled side of all animals, a short apex to bone distance was observed (Fig. 3A–C). Significant distance was observed for the drilled site of veh animals at 11 weeks that continued to increase over time (Fig. 3D, G, J, M, arrowheads). As expected, OPG-Fc and ZA at 11 weeks reduced periapical bone loss, reflected by shorter apex to bone distance (Fig. 3E, F, M). Discontinuation of OPG-Fc reversed this effect, evidenced by a significant increase of the apex to bone distance at 17 and 21 weeks (Fig. 3H, K, N, O, arrowheads). On the other hand, ZA discontinuation had no effect in periapical bone loss (Fig. 3I, L, N, O). Similar observations were found in maxillae with spontaneous periradicular bone loss. Both antiresorptive treatments

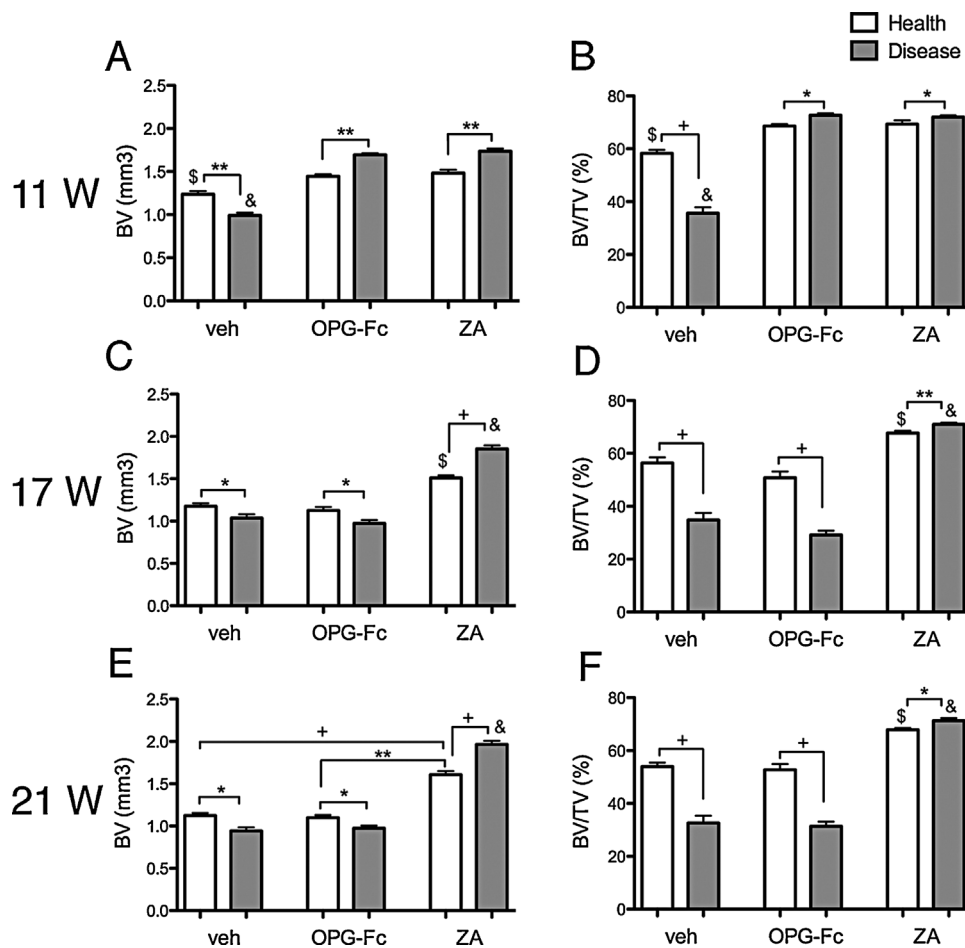


Fig. 6. Quantification of BV and BV/TV in the mandible of all mice. Eleven weeks of treatment (A, B) and 6 weeks (C, D) and 10 weeks (E, F) after drug discontinuation ($n = 16/\text{group}$ per period). $^{\$}$ Statistically significantly different compared with healthy mice, $p < 0.0001$. $^{\&}$ Statistically significantly different compared with diseased mice, $p < 0.0001$. $^{+}$ Statistically significantly different from indicated groups, $p < 0.0001$. ** Statistically significantly different from indicated groups, $p < 0.001$. * Statistically significantly different from indicated groups, $p < 0.05$.

attenuated alveolar bone loss at 11 weeks. Six and 10 weeks of OPG-Fc, but not ZA, discontinuation reversed the protection of alveolar bone loss that was similar to veh-treated mice (Supplemental Fig. S3).

Next, we examined changes of the PDL space width and lamina dura thickness at the furcation area of the mandibular molars.^(29,32) In nondrilled teeth of veh-, OPG-Fc-, and ZA-treated animals, a continuous PDL space and uniform lamina dura that increased in thickness with antiresorptive treatment were present (Fig. 4A–C, thin arrows and arrowheads). In the drilled side of veh-treated mice, there was increased width of the PDL space and loss of lamina dura that progressed over time (Fig. 4D, G, J, thin arrows and arrowheads, and Fig. 4M, P). Both antiresorptive treatments preserved PDL space width and thickened lamina dura at 11 weeks (Fig. 4E, F, M–R). OPG-Fc versus ZA discontinuation resulted in a significant reduction in the thickness of lamina dura and increase in PDL space width at 17 and 21 weeks (Fig. 4H, K, N, O, Q, R, thin arrows and arrowheads). ZA discontinuation had no effect compared with the week 11 measurements (Fig. 4I, L, N, O, Q, R).

The bone changes appeared to extend beyond the confines of the periodontal area to the adjacent alveolar

bone (Fig. 5). Significant osteolysis with exuberant expansion of the alveolar bone that increased over the time was noted in the diseased versus healthy site of veh mice (Fig. 5A, D, G, J, M–O, thin arrows). As previously reported,^(29,32) antiresorptive treatment inhibited bone osteolysis at 11 weeks (Fig. 5B, C, E, F, M), with an associated exuberant bone deposition on the buccal and palatal side of the alveolar ridge (Fig. 5B, C, E, F, M, arrowheads). Importantly, 6 and 10 weeks of OPG-Fc discontinuation reduced bone buccal and palatal thickness to levels similar to the veh group (Fig. 5). In contrast, ZA discontinuation had no effect on alveolar bone structure compared with the prediscontinuation levels (Fig. 5H, I, K, L, N, O). Similar findings were observed at the mandibular alveolar ridge (Supplemental Fig. S4).

Periapical disease decreased BV and BV/TV compared with the healthy site, and antiresorptives significantly increased BV and BV/TV compared with the veh group at 11 weeks. Significant increase in BV and BV/TV was observed between diseased versus healthy sites in OPG-Fc and ZA mice (Fig. 6A, B). OPG-Fc discontinuation decreased BV and BV/TV in the drilled site that returned to values similar to the veh group (Fig. 6C–F). In contrast, ZA discontinuation at 6 and 10 weeks

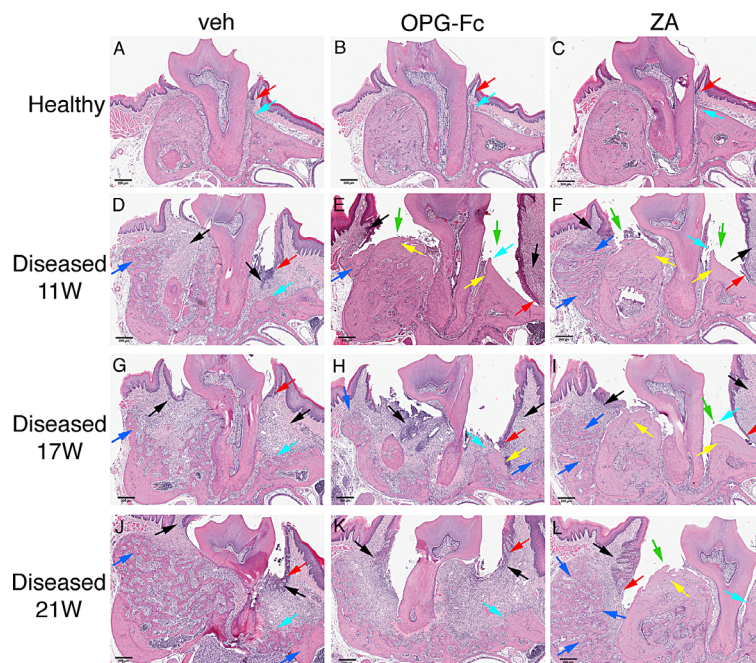


Fig. 7. Representative H&E-stained images from maxilla of all groups. (A–C) Healthy site of veh, OPG-Fc, and ZA animals. (D–F) Diseased site at 11 weeks at the end of antiresorptive treatment. (G–I) Diseased site of veh, OPG-Fc, and ZA 6 weeks after antiresorptive discontinuation. (J–L) Diseased site of veh, OPG-Fc, and ZA 10 weeks after antiresorptive discontinuation. Red arrows point to marginal gingival epithelium, turquoise arrows to alveolar crest, black arrows to areas of inflammation, blue arrows to periosteal bone deposition, yellow arrows to osteonecrotic areas, and green arrows to areas of bone exposure. Original magnification $\times 5$.

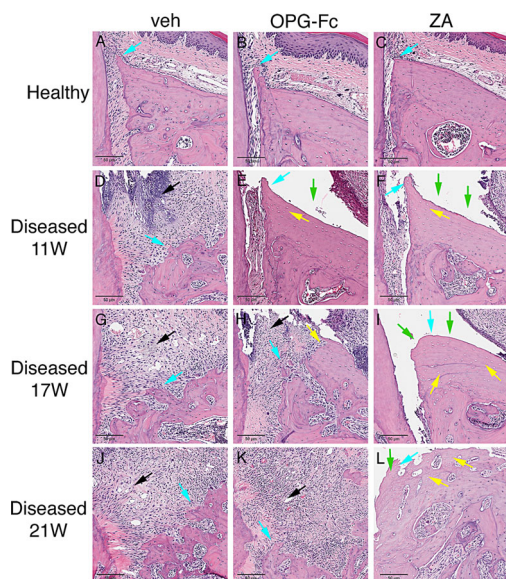


Fig. 8. Histologic appearance of periodontal and alveolar crest area of maxillae (A–C) Healthy site of veh, OPG-Fc, and ZA animals. (D–F) Diseased site at 11 weeks at the end of antiresorptive treatment. (G–I) Diseased site of veh, OPG-Fc, and ZA 6 weeks after antiresorptive discontinuation. (J–L) Diseased site of veh, OPG-Fc, and ZA 10 weeks after antiresorptive discontinuation. Turquoise arrows point to alveolar crest, black arrows to areas of inflammation, blue arrows to periosteal bone deposition, yellow arrows to osteonecrotic areas, and green arrows to areas of bone exposure. Original magnification $\times 10$.

had no effect on the BV and BV/TV levels (Fig. 6C–F). Similar observations were made for the BV and BV/TV values of the maxillae (Supplemental Fig. S5).

OPG-Fc but not ZA discontinuation reverses histologic features of ONJ

As reported,^(29,31,32) histologically healthy sites in all experimental groups and time points showed normal marginal epithelium (Fig. 7A–C; Fig. 8A–C, red arrows), PDL and alveolar bone (Fig. 7A–C; Fig. 8A–C, turquoise arrows). Abundant inflammatory infiltrate of the gingival and connective tissue (Fig. 7D, G, J, black arrows), severe destruction of the periradicular bone (Fig. 7D, G, J, turquoise arrows), migration of the marginal epithelium (Fig. 7D, G, J, red arrows), and bone expansion (Fig. 7D, G, J, blue arrows) were observed in the diseased site of veh-treated animals at all time points. Intense infiltration of inflammatory cells was noted in the diseased site of OPG-Fc- and ZA-treated mice at 11 weeks of treatment (Fig. 7E, F; Fig. 8E, F, black arrows); bone loss was present but appeared less compared with the veh animals (Fig. 7E, F; Fig. 8E, F, turquoise arrows). Empty osteocytic lacunae, areas of osteonecrosis (Fig. 7E, F; Fig. 8E, F, yellow arrows), and abundant periosteal bone formation (Fig. 7E, F; Fig. 8E, F, blue arrows) were found for both OPG-Fc and ZA mice. In several animals, necrotic bone was not covered by epithelium and was exposed to the oral cavity (Fig. 7E, F; Fig. 8E–F, green arrows; Table 1).

After OPG-Fc discontinuation, extensive osteolysis was noted in the maxillae, similar to the veh-treated animals (Fig. 7H, K; Fig. 8H, K). Importantly, areas of osteonecrosis and bone

exposed to the oral cavity significantly decreased by 6 weeks and were almost completely absent by 10 weeks of OPG-Fc discontinuation. Significant bone resorption and decreased areas of necrosis were associated with epithelial migration to areas of vital bone and with decreased number of animals with bone exposure (Fig. 7H, K; Fig. 8H, K; Table 1). In contrast, 6 and 10 weeks after ZA discontinuation did not alter these histologic features (Fig. 7I, L; Fig. 8I, L). Similar observations were made for healthy and drilled sites of the mandible for all experimental groups (Supplemental Fig. S6A–L).

In maxillae, increased marginal epithelium to alveolar bone crest (ABC) distance for diseased sites of veh animals at 11 weeks that continued to increase over time was found. As reported,^(29,31,32) antiresorptive treatment significantly decreased this distance because of reduced bone resorption (Fig. 9A–C). After OPG-Fc discontinuation, the epithelium to ABC distance progressively increased, as a result of increased bone resorption, and was statistically different compared with healthy sites or ZA-treated diseased sites (Fig. 9B). Six weeks after ZA discontinuation, the epithelium to ABC distance remained low and significantly different from the other groups (Fig. 9B). At 10 weeks after ZA discontinuation, an increase in the epithelium to ABC distance was noted but remained statistically different compared with the other groups (Fig. 9C). Similar results were found for the nondrilled and drilled sites of the mandible (Supplemental Fig. S7A–C). A significant increase in periosteal thickness was noted in the diseased versus healthy side for all treatment groups at all experimental time points. No consistent effects were noted by antiresorptive treatment or drug discontinuation (Fig. 9A–C).

The number of empty osteocytic lacunae (Fig. 9G–I) and osteonecrotic surface area (Fig. 9J–L) were measured in the

maxilla. No statistically significant presence of empty osteocytic lacunae was detected in healthy or diseased sites of veh mice or healthy sites of OPG-Fc or ZA mice at any time point. As previously reported,^(29,31,32) significant increases in empty osteocytic lacunae (Fig. 9G–I) and osteonecrotic area (Fig. 9J–L) were present in the diseased sites of mice on antiresorptive treatment at 11 weeks. Six and 10 weeks after OPG-Fc discontinuation, a significant reduction of empty osteocytic lacunae and osteonecrotic area was noted, to levels statistically similar to those of healthy sites and significantly lower than the diseased site of the ZA group. Interestingly, at 6 and 10 weeks after ZA discontinuation, significant increases in empty osteocytic lacunae number and osteonecrotic areas were observed. Comparable findings were observed for nondrilled and drilled sites of the mandible (Supplemental Fig. S7D–I).

Few TRAP+ cells were found at the healthy site of veh animals but were significantly increased at the diseased site of veh animals at all time points (Fig. 10A, D). TRAP+ cells were absent in OPG-Fc-treated animals in both healthy and diseased sites at 11 weeks (Fig. 10B, E, M). As previously reported,^(29,31,32) at 11 weeks TRAP+ cells in the diseased sites of ZA mice increased but demonstrated round morphology, with pyknotic nuclei, and were detached from the bone surface (Fig. 10C, F, M). After OPG-Fc discontinuation, TRAP+ cells in the diseased sites increased to higher levels than all other groups at 17 weeks and higher than the healthy sites of OPG-Fc animals at 21 weeks (Fig. 10H, K, N, O). A slight significant increase in TRAP+ cell number was found in the diseased sites after ZA discontinuation. Similar results were found for the nondrilled and drilled sites of the mandible (Supplemental Fig. S8A–O).

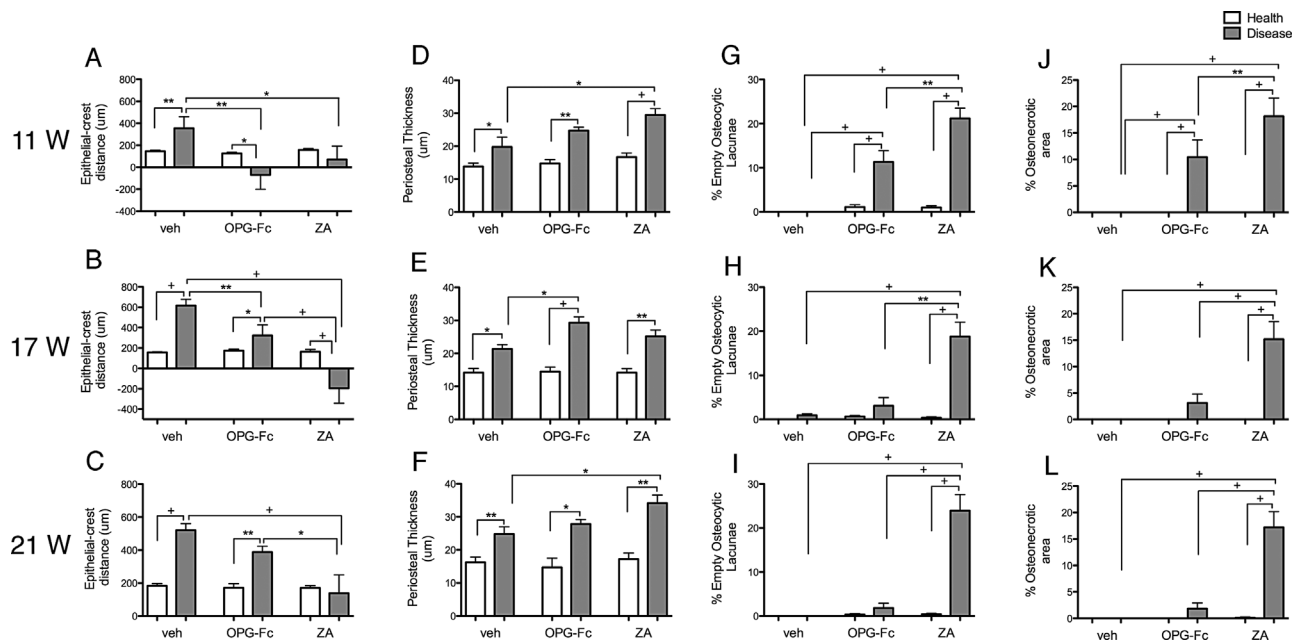


Fig. 9. Quantification of histologic findings. (A–C) The shortest epithelial-crest distance was determined. (D–F) Thickness of periosteum at the buccal side was measured. (G–I) Osteocytic lacunae were measured and empty lacunae were expressed as percent of total. (J–L) Area of osteonecrosis was measured and expressed as percent of total bone area ($n = 16/\text{group per period}$). +Statistically significantly different from indicated groups, $p < 0.0001$. **Statistically significantly different from indicated groups, $p < 0.001$. *Statistically significantly different from indicated groups, $p < 0.05$.

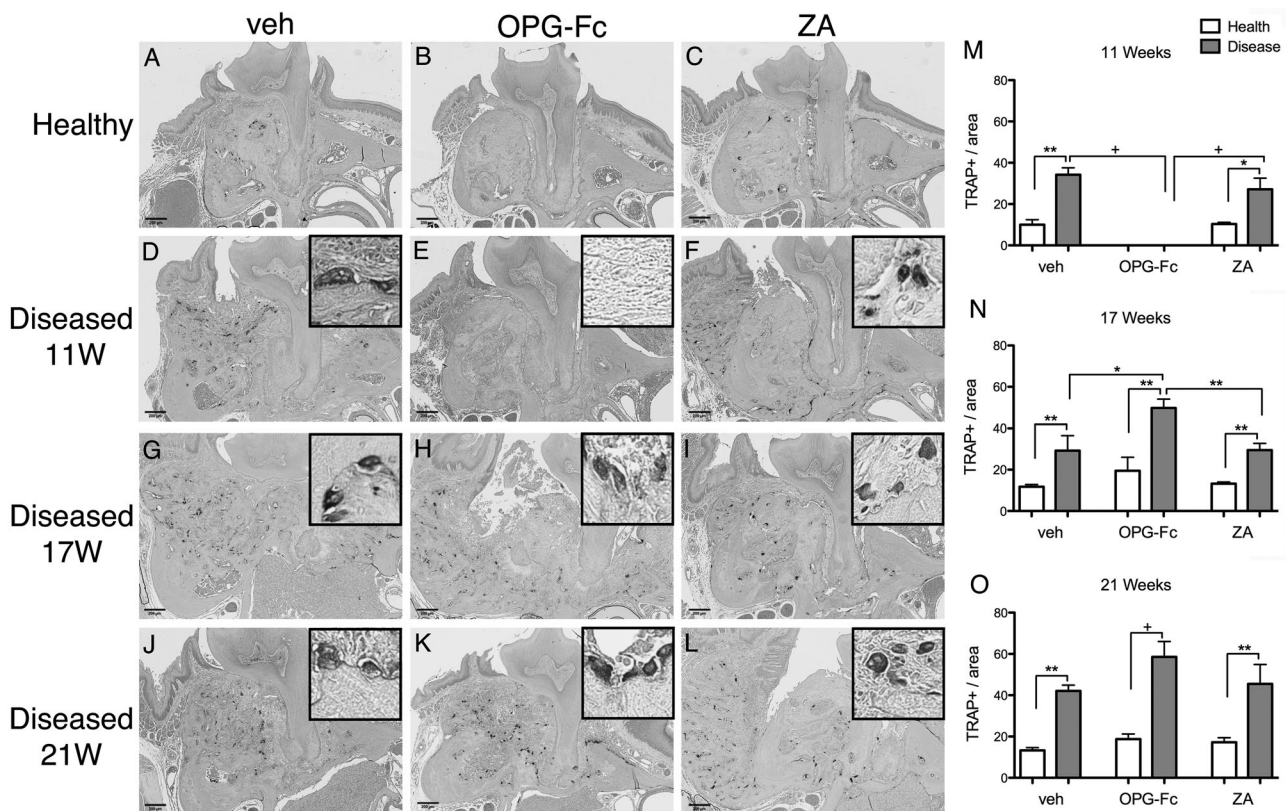


Fig. 10. Representative sections of the maxilla stained for TRAP+ cells (original magnification $\times 5$). Insets are magnified views of individual TRAP+ cells (original magnification $\times 20$). (A–C) Healthy site of veh, OPG-Fc, and ZA animals. (D–F) Diseased site at 11 weeks at the end of antiresorptive treatment. (G–I) Diseased site of veh, OPG-Fc, and ZA 6 weeks after antiresorptive discontinuation. (J–L) Diseased site of veh, OPG-Fc, and ZA 10 weeks after antiresorptive discontinuation. (M–O) Quantification of TRAP+ cell number ($n = 8/\text{group}$ per period). +Statistically significantly different from indicated groups, $p < 0.0001$. **Statistically significantly different from indicated groups, $p < 0.001$. *Statistically significantly different from indicated groups, $p < 0.05$.

Table 1 summarizes radiographic and histologic findings. Disease prevalence, which included periradicular and periapical disease, ranged from 47% to 64%, with no statistical differences among treatment groups or time points. Small areas of osteonecrosis were found in 2 veh-treated mice at 17 weeks and 1 at 21 weeks. Osteonecrosis was present in 75% of OPG-Fc and 63.4% of ZA animals at 11 weeks with no difference between antiresorptive groups but statistically different compared with veh. Bone exposure was observed only in animals on antiresorptives, ranging from 40.6% of the OPG-Fc and 52.6% of ZA-treated mice, respectively. After OPG-Fc discontinuation, areas of osteonecrosis and bone exposure were markedly diminished. Osteonecrosis incidence decreased to 42.1% and to 32.5% at 6 and 10 weeks after OPG-Fc discontinuation, respectively. Bone exposure decreased to 7.9% at 6 weeks after discontinuation. Importantly, at 10 weeks after OPG-Fc discontinuation, no animal with bone exposure was found. In contrast, 6 and 10 weeks of discontinuation in ZA-treated mice had no effect on incidence of osteonecrosis or bone exposure compared with prediscontinuation levels at 11 weeks.

To assess effects of antiresorptive discontinuation in other bones, we investigated radiographic changes in the femur of all

groups and time points. As expected, after 11 weeks of treatment, antiresorptives caused an increase in all bone radiographic indices including BV, BV/TV, trabecular number, and trabecular thickness. OPG-Fc induced a slightly higher trabecular thickness and smaller trabecular number compared with ZA. OPG-Fc discontinuation resulted in a progressive decrease in all measurements to veh levels. However, ZA discontinuation showed little effect and all radiographic indices remained high at both the 17- and 21-week time points (Fig. 11A–M).

To explore the effects of various treatments on osteoclast inhibition in femurs, TRAP+ cells were measured in the proximal femur. The number of TRAP+ cells in veh mice did not change over time (Fig. 11N, Q, T). At 11 weeks, no TRAP+ cells were observed in OPG-Fc mice (Fig. 11O), whereas increased TRAP+ cell numbers were found in ZA mice. However, in ZA mice, the osteoclasts had a round shape and were detached from the bone surface (Fig. 11P), with similar morphologic features as observed in the maxilla (Fig. 10) and mandible (Supplemental Fig. S8). At 6 and 10 weeks after OPG-Fc discontinuation, the number of TRAP+ cells significantly increased compared with the veh group (Fig. 11R, U, W). ZA discontinuation had no effect on TRAP+ cell numbers.

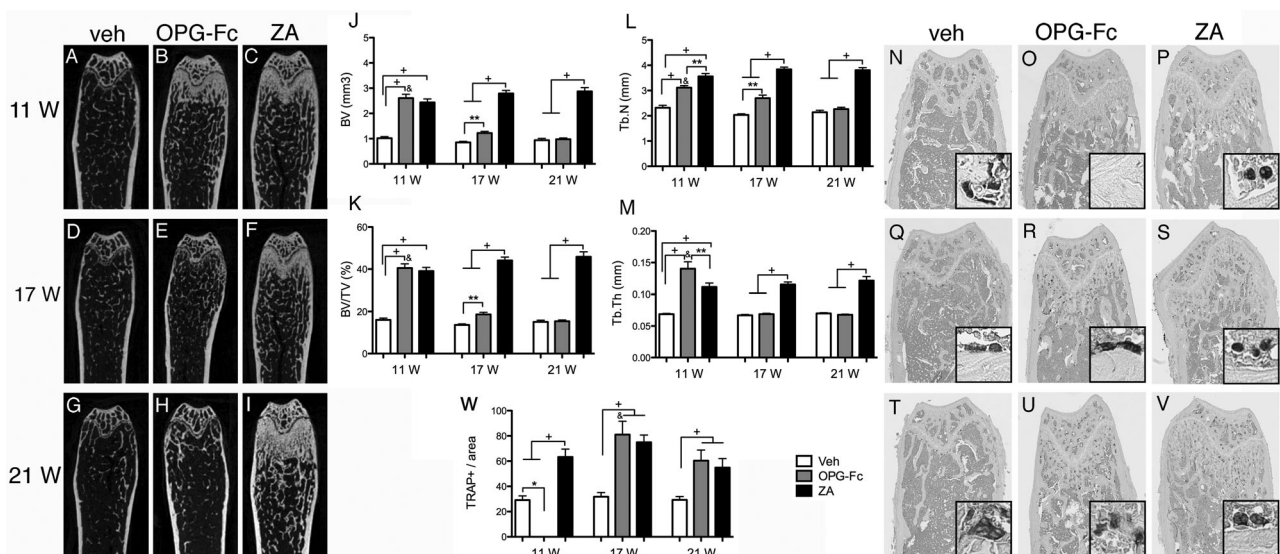


Fig. 11. Representative sagittal μ CT slices of femurs. (A–I) Veh, OPG-Fc, and ZA at the end of treatment and after drug discontinuation. (J–M) Quantification of BV, BV/TV, Tb.N, and Tb.Th ($n = 16$ /group per period). Representative sections of TRAP-stained sections from femurs (original magnification $\times 5$). Insets are magnified views of individual TRAP+ cells (original magnification $\times 20$). (N–P) Veh, OPG-Fc, and ZA animals at 11 weeks, (Q–S) 6 weeks after drug discontinuation, and (T–V) 10 weeks after drug discontinuation. (W) Quantification of TRAP+ cell number ($n = 8$ /group per period). & Statistically significantly different compared with diseased mice, $p < 0.0001$. + Statistically significantly different from indicated groups, $p < 0.0001$. ** Statistically significantly different from indicated groups, $p < 0.001$. * Statistically significantly different from indicated groups, $p < 0.05$.

Discussion

BPs are antiresorptive agents widely used in bone diseases with elevated osteoclastic activity, such as osteoporosis, cancer metastases to bone, multiple myeloma, and hypercalcemia of malignancy. Recently, the US FDA approved denosumab, an anti-RANKL monoclonal antibody, for the prevention of skeletal-related events in patients with bone metastases from solid tumors, for the management of unresectable giant cell tumors, for increasing bone mass in nonmetastatic prostate patients with androgen deprivation therapy, breast cancer patients receiving adjuvant aromatase inhibitor therapy, and men with osteoporosis, and for the treatment of postmenopausal and male osteoporosis.^(43–45) Although both BPs and denosumab target the osteoclast, their mechanism of function is distinctly different.

BPs have high affinity to bone surfaces, where they remain inactive until they are released during osteoclastic bone resorption.^(46–50) Because they target bones with high turnover, BP skeletal distribution is not homogeneous. The availability of exposed hydroxyapatite, blood supply, and the ratio of bone surface to bone volume are parameters that may contribute to this uneven distribution.⁽⁵¹⁾ On the other hand, denosumab, a high-affinity, highly specific monoclonal antibody for human RANKL, inhibits osteoclastic formation, function, and survival.^(52,53) Upon subcutaneous injection, denosumab is absorbed via the lymphatic system, with subsequent drainage into the vasculature. Three phases of drug distribution are described: a prolonged absorption phase with maximum serum concentration at 5 to 21 days, a long duration phase with a 32-day maximum half-life, and a rapid terminal phase when serum concentrations reach levels below 1000 ng/mL.^(54,55)

Given their distinct biodistribution and mechanism of action, BP versus denosumab inhibition of osteoclastic function has distinct temporal dynamics. Because of their incorporation in the bone mineral, BPs can exert their anti-osteoclastic effects long after their administration.⁽⁴⁶⁾ In contrast, denosumab does not require binding to bone mineral to exert its anti-osteoclastic activity⁽³⁰⁾ and demonstrates rapid reversibility of its antiresorptive effects.⁽⁴³⁾

Here, we investigated osteoclast recovery by measuring serum TRACP-5b levels before and at various times after antiresorptive discontinuation. As expected, ZA treatment significantly attenuated TRACP-5b levels. After ZA discontinuation, TRACP-5b levels gradually returned to baseline, remaining lower than the veh group for up to 6 weeks and reaching veh group levels by 10 weeks after drug withdrawal. These findings resemble data from the FLEX randomized trial showing that in osteoporotic patients receiving alendronate for 5 years, BP discontinuation results in a gradual increase of serum bone resorption and formation markers measured at 3 and 5 years after discontinuation.⁽⁵⁶⁾ A faster recovery of bone turnover markers is reported at 1 year after BP discontinuation in osteoporotic patients receiving risedronate for 3 years.⁽⁵⁷⁾ The HORIZON-Pivotal Fracture Trial (PFT) reported that annual ZA infusions are efficacious in decreasing bone turnover and reducing fracture risk in postmenopausal women with osteoporosis.⁽⁵⁸⁾ Interestingly, in the HORIZON extension, discontinuation of iv ZA infusions for a period of 36 months showed that bone turnover markers increase only slightly compared with controls continuing to receive ZA.⁽⁵⁹⁾ These variations in resolution of bone turnover indices after BP discontinuation could reflect differences in BP biodistribution, bone mineral affinity, and mode of administration.

The RANKL inhibitor OPG-Fc was used as a surrogate to denosumab because the latter does not recognize the mouse RANKL.⁽³⁰⁾ OPG-Fc treatment significantly reduced serum TRACP-5b levels that declined to levels lower than veh- or ZA-treated animals. Interestingly, at 4 and 6 weeks after OPG-Fc discontinuation, TRACP-5b levels rose above those in the veh-treated group and declined to baseline by 10 weeks. These results parallel observations from studies in postmenopausal patients with osteoporosis, wherein denosumab discontinuation led to recovery of bone resorption markers that transiently exceeded pretreatment levels before recovering to normal.⁽⁶⁰⁾ At the tissue level, denosumab treatment reduces bone turnover, including eroded surfaces and tetracycline labeling.^(61,62) After denosumab cessation, bone histomorphometry indices return to pretreatment levels, indicating that the effects of denosumab on bone turnover are fully reversible.⁽⁶³⁾

Given the great importance of osteoclasts in bone healing and in periapical and periodontal disease progression^(64–67) and the central role of bone remodeling suppression in ONJ pathophysiology,^(5,11,12) discontinuation of oral bisphosphonates in patients with low bone turnover marker values was recommended to allow recovery of osteoclastic function before dental surgical procedures.⁽⁶⁸⁾ However, such recommendations have been questioned, and the significance of oral bisphosphonate discontinuation in the management of the ONJ patient remains controversial.⁽⁶⁹⁾

Recommendations for discontinuation of antiresorptive medication by professional organizations are cautious and based on theoretical assumptions. For osteoporotic patients, the American Dental Association (ADA) Council on Scientific Affairs recommends that before a dental procedure, “discontinuation of antiresorptive therapy should be a medical decision based primarily on the risk of experiencing SRE secondary to low bone density, not the potential risk of developing ARONJ.”⁽¹⁵⁾ The AAOMS position paper reports that a theoretical benefit might exist for patients with history of prolonged bisphosphonate treatment (>4 years),⁽⁷⁾ whereas the International Task Force opines that “it may be advisable to stop antiresorptive therapy if it is possible to do so without adverse consequences for bone health.”⁽⁸⁾ Similarly, recommendations for patients receiving oncologic doses of antiresorptives on drug discontinuation before surgical dental procedures are inconclusive. For patients who have developed ONJ, discontinuation of antiresorptive medication until closure of the soft tissue defect with well-epithelialized mucosa may be considered, depending on the systemic disease status. A potentially greater rate of ONJ resolution upon discontinuation of denosumab (40.4%) versus ZA (29.7%) in cancer patients with bone metastases has been reported.⁽⁷⁰⁾ However, the benefit of such drug discontinuation in ONJ healing is unclear. All reports uniformly describe the lack of evidence to support or contradict utilization of drug withdrawal in the management of patients on antiresorptives and emphasize the great importance of studies that would inform such clinical decisions.^(7,8,70)

To address this void in our understanding of ONJ management as it pertains to drug holidays for resolution of existing ONJ lesions, we treated mice with high-dose OPG-Fc to inhibit RANKL-RANK signaling or with ZA to develop ONJ lesions and then discontinued drug administration for 6 or 10 weeks. Qualitative and quantitative radiographic and histologic analysis of mandibles and maxillae revealed that both antiresorptive treatments successfully induced ONJ-like lesions in mice, similar to our previous observations.^(29,31,32) Upon discontinuation of OPG-Fc, radiographic indices of alveolar bone loss, such as PDL

space width, lamina dura loss, and alveolar BV and BV/TV, were similar to the veh-treated animals. However, ZA cessation did not significantly alter radiographic appearance within the experimental time frame. Importantly, OPG-Fc discontinuation progressively decreased histologic features of ONJ, including number of empty osteocytic lacunae, osteonecrotic area, and presence of exposed bone. In contrast, for both time points of ZA, all histologic indices of ONJ remained similar to the prewithdrawal levels and different than both the veh and OPG-Fc groups. An interesting caveat that our studies did not address is whether ONJ incidence and severity would have progressed if antiresorptives were continuously present for the 21 weeks of the experiment. Thus, although it remained the same pre- and post-ZA withdrawal, ONJ burden could have potentially worsened if ZA were continuously present. If that were true, ZA withdrawal would have ablated this increased burden.

The reversal of ONJ radiographic and histologic findings after OPG-Fc discontinuation was paralleled by a robust recovery of osteoclastic function, indicated by the increased serum TRACP-5b levels and the increased osteoclast numbers in the femur and the diseased sites of the mandible and maxillae. Because OPG-Fc withdrawal was associated with bone loss that progressively reached similar levels to that of veh animals and with increased osteoclast numbers and activity, the reduction in osteonecrotic areas appears to be mainly attributable to removal of the necrotic bone by the recovered osteoclasts. Increased bone remodeling, although probably present in areas of inflammation, appeared less likely to play a significant role in the reduced bone necrosis and exposure.

The close association of osteoclastic recovery to ONJ burden points to the central involvement of osteoclastic function, not only for ONJ pathogenesis but also, importantly, for ONJ resolution. Our data collectively demonstrate that OPG-Fc, but not ZA, discontinuation reversed radiographic and histologic features of osteonecrosis and support theoretical predictions based on antiresorptive pharmacokinetics and mode of action hypothesizing that denosumab withdrawal leads to higher recovery rates of ONJ compared with ZA because of denosumab’s reversible inhibition of osteoclastic activity.^(70,71) Although our findings are potentially instructive for other settings of drug holidays, such as before tooth extractions or oral surgical interventions, future studies that directly address these scenarios would provide valuable insight into usefulness of antiresorptive withdrawal to prevent ONJ development.

In conclusion, we report that antiresorptive treatment discontinuation alters radiographic and histologic findings of ONJ in mice differently, depending on the type of antiresorptive agent. To the best of our knowledge, this is the first experimental study to illustrate and quantify such differences. Our findings provide a rationale that informs clinical decisions for drug holidays in the management of the ONJ patient. Indeed, if our findings remain translatable to the clinical setting, they would suggest that for patients receiving high-dose antiresorptives for the management of malignancy, denosumab discontinuation would offer faster and more complete resolution of ONJ compared with BPs.

Disclosures

ST has served as a paid consultant for and has received grant support from Amgen Inc. PK, RB, and DD are full-time employees and/or shareholders of Amgen Inc. All other authors state that they do not have any conflicts of interest.

Acknowledgments

This work was supported by grants from Amgen Inc, and by NIH/NIDCR R01 DE019465. RSM was supported by fellowships from the State of Sao Paulo Research Foundation (FAPESP) #2012/09968-5, the Coordination for the Improvement of Higher Level or Education Personnel (CAPES) #11575/13-1, and Lemann Foundation.

Authors' roles: Conceived and designed the experiments: RSM, FQP, SMD, PK, RWB, TLA, and ST. Performed the experiments: RSM, HS, OB, FQP, SDM, PK, DD, TLA, and ST. Analyzed the data: RSM, HS, PK, RWB, TLA, and ST. Contributed to the writing of the manuscript: RSM and ST. Contributed to editing the manuscript: RSM, HS, OB, FQP, SMD, PK, RWB, DD, TLA, and ST.

References

1. Tolia M, Zygogianni A, Kouvaris JR, et al. The key role of bisphosphonates in the supportive care of cancer patients. *Anticancer Res.* 2014;34:23–37.
2. Tella SH, Gallagher JC. Prevention and treatment of postmenopausal osteoporosis. *J Steroid Biochem Mol Biol.* 2014;142:155–70.
3. Morgans AK, Smith MR. Bone-targeted agents: preventing skeletal complications in prostate cancer. *Urol Clin North Am.* 2012;39:533–46.
4. Roelofs AJ, Thompson K, Gordon S, Rogers MJ. Molecular mechanisms of action of bisphosphonates: current status. *Clin Cancer Res.* 2006;12:2225–30s.
5. Allen MR, Ruggiero SL. A review of pharmaceutical agents and oral bone health: how osteonecrosis of the jaw has affected the field. *Int J Oral Maxillofac Implants.* 2014;29:e45–57.
6. Khosla S, Burr D, Cauley J, et al. Bisphosphonate-associated osteonecrosis of the jaw: report of a task force of the American Society for Bone and Mineral Research. *J Bone Miner Res.* 2007;22:1479–91.
7. Ruggiero SL, Dodson TB, Fantasia J, et al. Medication-related osteonecrosis of the jaw-2014 update [Internet]. American Association of Oral and Maxillofacial Surgeons position paper. 2014. Available at: http://www.aaoms.org/docs/position_papers/mronj_position_paper.pdf?pdf=MRONJ-Position-Paper.
8. Khan A., Morrison A, Hanley D, et al. Diagnosis and management of osteonecrosis of the jaw: a systematic review and international consensus. *J Bone Miner Res.* 2015;30:3–23.
9. Marx RE. Pamidronate (Aredia) and zoledronate (Zometa) induced avascular necrosis of the jaws: a growing epidemic. *J Oral Maxillofac Surg.* 2003;61:1115–7.
10. Ruggiero SL, Mehrotra B, Rosenberg TJ, Engroff SL. Osteonecrosis of the jaws associated with the use of bisphosphonates: a review of 63 cases. *J Oral Maxillofac Surg.* 2004;62:527–34.
11. Yamashita J, McCauley LK. Antiresorptives and osteonecrosis of the jaw. *J Evid Based Dent Pract.* 2012;12:233–47.
12. Allen MR, Burr DB. The pathogenesis of bisphosphonate-related osteonecrosis of the jaw: so many hypotheses, so few data. *J Oral Maxillofac Surg.* 2009;67:61–70.
13. Allen MR. Bisphosphonates and osteonecrosis of the jaw: moving from the bedside to the bench. *Cells Tissues Organs.* 2009;189:289–94.
14. Woo SB, Hellstein JW, Kalmar JR. Narrative [corrected] review: bisphosphonates and osteonecrosis of the jaws. *Ann Intern Med.* 2006;144:753–61.
15. Hellstein JW, Adler RA, Edwards B, et al. Managing the care of patients receiving antiresorptive therapy for prevention and treatment of osteoporosis: executive summary of recommendations from the American Dental Association Council on Scientific Affairs. *J Am Dent Assoc.* 2011;142:1243–51.
16. Damm DD, Jones DM. Bisphosphonate-related osteonecrosis of the jaws: a potential alternative to drug holidays. *Gen Dent.* 2013;61:33–8.
17. Food and Drug Administration. Background document of meeting of Advisory Committee for Reproductive Health Drugs and Drug Safety and Risk Management Advisory Committee [Internet]. 2011. Available at: <http://www.fda.gov/downloads/AdvisoryCommittees/CommitteesMeetingMaterials/drugs/DrugSafetyandRiskManagementAdvisoryCommittee/ucm270958.pdf>.
18. Abtahi J, Agholme F, Sandberg O, Aspenberg P. Bisphosphonate-induced osteonecrosis of the jaw in a rat model arises first after the bone has become exposed. No primary necrosis in unexposed bone. *J Oral Pathol Med.* 2012;41:494–9.
19. Aghaloo TL, Kang B, Sung EC, et al. Periodontal disease and bisphosphonates induce osteonecrosis of the jaws in the rat. *J Bone Miner Res.* 2011;26:1871–82.
20. Aguirre JI, Akhter MP, Kimmel DB, et al. Oncologic doses of zoledronic acid induce osteonecrosis of the jaw-like lesions in rice rats (*Oryzomys palustris*) with periodontitis. *J Bone Miner Res.* 2012;27:2130–43.
21. Ali-Erdem M, Burak-Cankaya A, Cemil-Isler S, et al. Extraction socket healing in rats treated with bisphosphonate: animal model for bisphosphonate related osteonecrosis of jaws in multiple myeloma patients. *Med Oral Patol Oral Cir Bucal.* 2011;16:e879–83.
22. Bi Y, Gao Y, Ehrirchiou D, et al. Bisphosphonates cause osteonecrosis of the jaw-like disease in mice. *Am J Pathol.* 2010;177:280–90.
23. Lopez-Jornet P, Camacho-Alonso F, Molina-Minano F, Gomez-Garcia F, Vicente-Ortega V. An experimental study of bisphosphonate-induced jaws osteonecrosis in Sprague-Dawley rats. *J Oral Pathol Med.* 2010;39:697–702.
24. Kikuri T, Kim I, Yamaza T, et al. Cell-based immunotherapy with mesenchymal stem cells cures bisphosphonate-related osteonecrosis of the jaw-like disease in mice. *J Bone Miner Res.* 2010;25:1668–79.
25. Sonis ST, Watkins BA, Lyng GD, Lerman MA, Anderson KC. Bony changes in the jaws of rats treated with zoledronic acid and dexamethasone before dental extractions mimic bisphosphonate-related osteonecrosis in cancer patients. *Oral Oncol.* 2009;45:164–72.
26. Pautke C, Kreutzer K, Weitz J, et al. Bisphosphonate related osteonecrosis of the jaw: a minipig large animal model. *Bone.* 2012;51:592–9.
27. Allen MR, Chu TM, Ruggiero SL. Absence of exposed bone following dental extraction in beagle dogs treated with 9 months of high-dose zoledronic acid combined with dexamethasone. *J Oral Maxillofac Surg.* 2013;71:1017–26.
28. Gotcher JE, Jee WS. The progress of the periodontal syndrome in the rice cat. II. The effects of a diphosphonate on the periodontium. *J Periodontol Res.* 1981;16:441–55.
29. Kang B, Cheong S, Chaichanasakul T, et al. Periapical disease and bisphosphonates induce osteonecrosis of the jaws in mice. *J Bone Miner Res.* 2013;28:1631–40.
30. Kostenuik PJ, Nguyen HQ, McCabe J, et al. Denosumab, a fully human monoclonal antibody to RANKL, inhibits bone resorption and increases BMD in knock-in mice that express chimeric (murine/human) RANKL. *J Bone Miner Res.* 2009;24:182–95.
31. de Molon RS, Cheong S, Bezouglaia O, et al. Spontaneous osteonecrosis of the jaws in the maxilla of mice on antiresorptive treatment: a novel ONJ mouse model. *Bone.* 2014;68:11–9.
32. Aghaloo TL, Cheong S, Bezouglaia O, et al. RANKL inhibitors induce osteonecrosis of the jaw in mice with periapical disease. *J Bone Miner Res.* 2014;29:843–54.
33. Williams DW, Lee C, Kim T, et al. Impaired bone resorption and woven bone formation are associated with development of osteonecrosis of the jaw-like lesions by bisphosphonate and anti-receptor activator of NF-kappaB ligand antibody in mice. *Am J Pathol.* 2014;184:3084–93.
34. Lacey DL, Boyle WJ, Simonet WS, et al. Bench to bedside: elucidation of the OPG-RANK-RANKL pathway and the development of denosumab. *Nat Rev Drug Discov.* 2012;11:401–19.
35. Kostenuik PJ, Smith SY, Jolette J, Schroeder J, Pyrah I, Ominsky MS. Decreased bone remodeling and porosity are associated with improved bone strength in ovariectomized cynomolgus monkeys

- treated with denosumab, a fully human RANKL antibody. *Bone*. 2011;49:151–61.
36. Sasaki H, Hou L, Belani A, et al. IL-10, but not IL-4, suppresses infection-stimulated bone resorption in vivo. *J Immunol*. 2000; 165:3626–30.
 37. Wang CY, Stashenko P. Kinetics of bone-resorbing activity in developing periapical lesions. *J Dent Res*. 1991;70:1362–6.
 38. Lawson GW. Etiopathogenesis of mandibulofacial and maxillofacial abscesses in mice. *Comp Med*. 2010;60:200–4.
 39. Clarke MC, Taylor RJ, Hall GA, Jones W. The occurrence in mice of facial and mandibular abscesses associated with *Staphylococcus aureus*. *Lab Anim*. 1978;12:121–3.
 40. Grant N, Jackson K, Lee R, Scharf B. Mandibular mass in a young Swiss-Webster mouse. *Lab Anim (NY)*. 2002;31:25–6.
 41. Bouxsein ML, Boyd SK, Christiansen BA, Guldberg RE, Jepsen KJ, Muller R. Guidelines for assessment of bone microstructure in rodents using micro-computed tomography. *J Bone Miner Res*. 2010;25:1468–86.
 42. Ominsky MS, Li X, Asuncion FJ, et al. RANKL inhibition with osteoprotegerin increases bone strength by improving cortical and trabecular bone architecture in ovariectomized rats. *J Bone Miner Res*. 2008;23:672–82.
 43. Silva I, Branco JC. Denosumab: recent update in postmenopausal osteoporosis. *Acta Reumatol Port*. 2012;37:302–13.
 44. Iranikhan M, Stricker S, Freeman MK. Future of bisphosphonates and denosumab for men with advanced prostate cancer. *Cancer Manag Res*. 2014;6:217–24.
 45. Lewin J, Thomas D. Denosumab: a new treatment option for giant cell tumor of bone. *Drugs Today (Barc)*. 2013;49:693–700.
 46. Kimmel DB. Mechanism of action, pharmacokinetic and pharmacodynamic profile, and clinical applications of nitrogen-containing bisphosphonates. *J Dent Res*. 2007;86:1022–33.
 47. Coxon FP, Helfrich MH, Van't Hof R, et al. Protein geranylgeranylation is required for osteoclast formation, function, and survival: inhibition by bisphosphonates and GGTI-298. *J Bone Miner Res*. 2000;15: 1467–76.
 48. Hughes DE, Wright KR, Uy HL, et al. Bisphosphonates promote apoptosis in murine osteoclasts in vitro and in vivo. *J Bone Miner Res*. 1995;10:1478–87.
 49. Fisher JE, Rogers MJ, Halasy JM, et al. Alendronate mechanism of action: geranylgeraniol, an intermediate in the mevalonate pathway, prevents inhibition of osteoclast formation, bone resorption, and kinase activation in vitro. *Proc Natl Acad Sci USA*. 1999;96:133–8.
 50. Luckman SP, Hughes DE, Coxon FP, Graham R, Russell G, Rogers MJ. Nitrogen-containing bisphosphonates inhibit the mevalonate pathway and prevent post-translational prenylation of GTP-binding proteins, including Ras. *J Bone Miner Res*. 1998;13:581–9.
 51. Lin JH. Bisphosphonates: a review of their pharmacokinetic properties. *Bone*. 1996;18:75–85.
 52. Romas E. Clinical applications of RANKL-inhibition. *Intern Med J*. 2009;39:110–6.
 53. Geusens P. Emerging treatments for postmenopausal osteoporosis—focus on denosumab. *Clin Interv Aging*. 2009;4:241–50.
 54. Lewiecki EM. Denosumab: an investigational drug for the management of postmenopausal osteoporosis. *Biologics*. 2008; 2:645–53.
 55. Lewiecki EM. Denosumab update. *Curr Opin Rheumatol*. 2009;21: 369–73.
 56. Black DM, Schwartz AV, Ensrud KE, et al. Effects of continuing or stopping alendronate after 5 years of treatment: the Fracture Intervention Trial Long-term Extension (FLEX): a randomized trial. *JAMA*. 2006;296:2927–38.
 57. Watts NB, Chines A, Olszynski WP, et al. Fracture risk remains reduced one year after discontinuation of risedronate. *Osteoporos Int*. 2008;19:365–72.
 58. Black DM, Delmas PD, Eastell R, et al. Once-yearly zoledronic acid for treatment of postmenopausal osteoporosis. *N Engl J Med*. 2007;356:1809–22.
 59. Black DM, Reid IR, Boonen S, et al. The effect of 3 versus 6 years of zoledronic acid treatment of osteoporosis: a randomized extension to the HORIZON-Pivotal Fracture Trial (PFT). *J Bone Miner Res*. 2012;27:243–54.
 60. Bone HG, Bolognese MA, Yuen CK, et al. Effects of denosumab treatment and discontinuation on bone mineral density and bone turnover markers in postmenopausal women with low bone mass. *J Clin Endocrinol Metab*. 2011;96:972–80.
 61. Brown JP, Reid IR, Wagman RB, et al. Effects of up to 5 years of denosumab treatment on bone histology and histomorphometry: the FREEDOM study extension. *J Bone Miner Res*. 2014;29:2051–6.
 62. Reid IR, Miller PD, Brown JP, et al. Effects of denosumab on bone histomorphometry: the FREEDOM and STAND studies. *J Bone Miner Res*. 2010;25:2256–65.
 63. Brown JP, Dempster DW, Ding B, et al. Bone remodeling in postmenopausal women who discontinued denosumab treatment: off-treatment biopsy study. *J Bone Miner Res*. 2011;26: 2737–44.
 64. Han X, Lin X, Yu X, et al. *Porphyromonas gingivalis* infection-associated periodontal bone resorption is dependent on receptor activator of NF- κ B ligand. *Infect Immun*. 2013;81: 1502–9.
 65. Yuan H, Gupte R, Zelkha S, Amar S. Receptor activator of nuclear factor κ B ligand antagonists inhibit tissue inflammation and bone loss in experimental periodontitis. *J Clin Periodontol*. 2011;38:1029–36.
 66. Jin Q, Cirelli JA, Park CH, et al. RANKL inhibition through osteoprotegerin blocks bone loss in experimental periodontitis. *J Periodontol*. 2007;78:1300–8.
 67. Xiong H, Wei L, Hu Y, Zhang C, Peng B. Effect of alendronate on alveolar bone resorption and angiogenesis in rats with experimental periapical lesions. *Int Endod J*. 2010;43:485–91.
 68. Marx RE, Cillo JE Jr, Ulloa JJ. Oral bisphosphonate-induced osteonecrosis: risk factors, prediction of risk using serum CTX testing, prevention, and treatment. *J Oral Maxillofac Surg*. 2007;65:2397–410.
 69. American Society for Bone and Mineral Research Task Force on Osteoporosis of the Jaw, Khosla S, Burr D, et al. Oral bisphosphonate-induced osteonecrosis: risk factors, prediction of risk using serum CTX testing, prevention, and treatment. *J Oral Maxillofac Surg*. 2008;66:1320–1; author reply 1321–2.
 70. Saad F, Brown JE, Van Poznak C, et al. Incidence, risk factors, and outcomes of osteonecrosis of the jaw: integrated analysis from three blinded active-controlled phase III trials in cancer patients with bone metastases. *Ann Oncol*. 2012;23:1341–7.
 71. Malan J, Ettinger K, Naumann E, Beirne OR. The relationship of denosumab pharmacology and osteonecrosis of the jaws. *Oral Surg Oral Med Oral Pathol Oral Radiol*. 2012;114:671–6.